Eur. Radiol. 8, 175–188 (1998)

Neuroradiology European Radiology

Review article

Imaging of the normal and pathological orbit

B. Duvoisin[1], **F. E. Zanella**[2], **K. W. Sievers**[3]

[1] Department of Radiology, University of Lausanne, CH-1011 Lausanne, Switzerland
[2] Department of Neuroradiology, University of Frankfurt, Frankfurt am Main, Germany
[3] Department of Diagnostic Radiology, University of Rostock, Rostock, Germany

Received 15 April 1996; Revision received 19 June 1997; Accepted 20 June 1997

Abstract. Computerized techniques (CT and MRI) allow precise delineation of orbital anatomy and abnormalities. Orbital tumors are nicely depicted by these methods; various examples are illustrated in this article, with discussion of the respective impact of CT and MRI. Orbital inflammation and foreign bodies usually represent radiologic emergencies, prompting use of CT (frequently) or MRI (occasionally). Digital subtraction angiography (DSA) is indicated for diagnosis of vascular changes (mainly carotid-cavernous fistula, aneurysms, angiomas, Rendu-Osler disease). Angiography is usually done to ascertain the possibility of an interventional procedure. Orbital vascular interventions include re-canalization of occluded vessels, and embolization of pathologic (tumorous or post-traumatic) vessels.

Key words: Orbit – CT – MRI – Angiography – Orbital tumors – Orbital inflammation – Orbital foreign bodies – Endovascular procedures

Normal anatomy

In former times conventional radiography was able to visualize only the bony structures of the orbit. Therefore, only bony tumors or destruction, fractures, or radiodense foreign bodies were visible. The new computerized techniques introduced from the early 70s onwards allowed the anatomic delineation of soft tissue structures. Now not only the bony but also the soft tissue parts of the orbit such as the globe, muscles, nerves and vessels are routinely visible by the new modalities of computed tomography (CT) and magnetic resonance imaging (MRI). The major goal of these techniques is the two-dimensional evaluation of the orbit, free of any superimposing structures. With spiral CT, CT has entered the multiplanar domain, as excellent two-dimensional reconstructions in any plane are possible; furthermore, spiral CT allows three-dimensional reconstructions, which provide more information for clinical diagnoses, as well as for surgical management [1]. MRI does not use ionizing radiation, and is capable of changing slice orientation without repositioning the patient.

Angiography has also been improved by computerized technology; digital subtraction angiography (DSA) allows the delineation of even small branches of the arteries without any loss of information from superimposing parts of the base of the skull.

This knowledge of the two-dimensional anatomy, and of the vascular anatomy, is essential for diagnosing pathological changes of the orbit.

Bony structures

Contrast between bone and surrounding soft tissues is higher on CT than on MRI. The walls of the orbit consist of dense cortical bone which significantly attenuates the X-ray beam, and are therefore clearly delineated on CT from soft tissues. However, because bone lacks mobile hydrogen protons and thus, on MRI, there is subsequent absence of signal, it is less precisely delimitable from adjacent soft tissues.

Routinely the orbit should be examined by contiguous CT sections with a thickness of 2–4 mm. Although 2-mm slice thickness produces high-quality images, thicker slices provide adequate resolution for small structures with fewer sections. Furthermore, ideally the image data should be reconstructed two times – once with a high resolution bone algorithm and once with a soft tissue algorithms – as the image quality is not optimal if only the window settings are changed. As regards slice orientation, axial and coronal sections are recommended. Axial sections (Fig. 1) are obtained parallel to the infraorbito-meatal line, which is close to the course of the optic canal. Supine positioning of the patient and an axial slice orientation minimize movement artifacts,

Correspondence to: B. Duvoisin

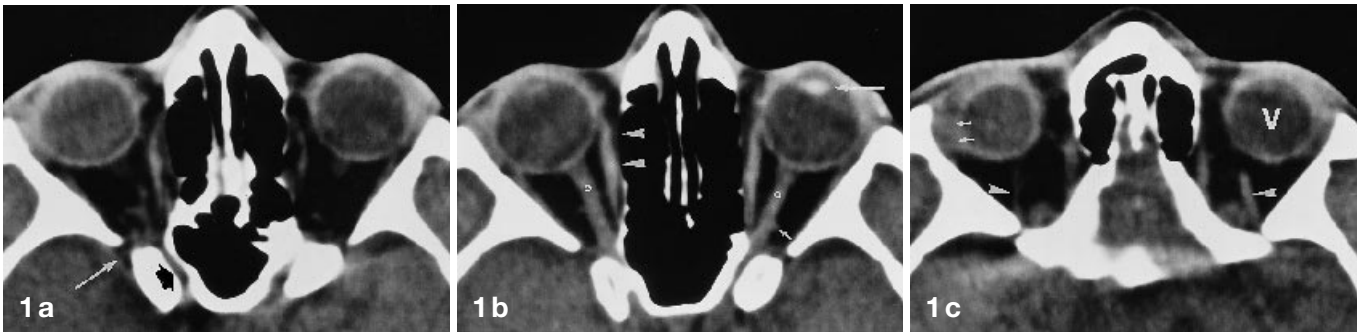

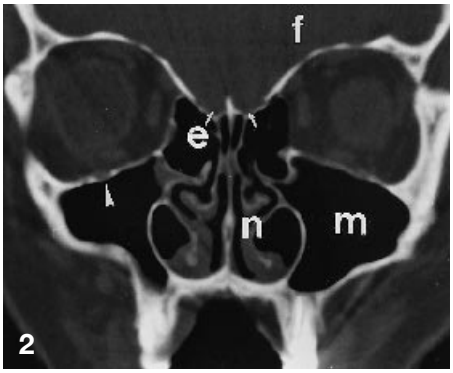

Fig. 1 a–c. Axial CT scans (slice thickness 2 mm, soft tissue setting). **a** Section below the level of the lens. There is good delineation of the bony and soft tissue structures including the ethmoidal sinus, superior orbital fissure *(white arrow),* and optic canal *(black arrow).* **b** Mid-section of the lens *(large white arrow).* The lamina papyracea *(white arrowheads),* optic nerves *(small circles),* and ophthalmic artery *(small white arrow)* are seen. **c** Lacrimal gland *(small white arrows)* next to the globe *(v),* and the superior ophthalmic vein *(arrowheads)*

Fig. 2. Coronal CT scan (slice thickness 2 mm, bone setting). There is excellent visualization of the roof and the floor of the orbit together with the maxillary *(m)* and ethmoidal sinuses *(e).* The infraorbital fissure *(white arrowhead),* nasal cavity *(n)*, and frontal base of ths skull *(f)* with olfactory groove *(small white arrows)* are also seen

as well as artifacts from dental work. Coronal sections (Fig. 2) are either reformatted from axial data obtained with spiral CT or, if spiral CT is unavailable, obtained directly in the prone or supine position.

The thin floor of the orbit, as a part of the maxilla, zygomatic, and palatine bones, borders the maxillary sinus and contains the infraorbital canal and nerve in its anterior part. The medial wall is represented by the lacrymal and orbital plate of the ethmoid (or lamina orbitalis). In the lower aspect, it contains a bony canal, 2 cm long, draining into the inferior nasal cavity: the nasolacrimal duct. The lateral wall is formed by the zygomatic bone and the greater wing of the sphenoid. The roof of the orbit is composed of the frontal bone and the lesser wing of the sphenoid, bordering the frontal sinus. In the superolateral part of the orbit, a bony fossa contains the lacrimal gland. The superior and inferior orbital fissures are formed by the greater and lesser wings of the sphenoid, and the maxilla, respectively (Fig. 1 a). Furthermore, the optic canal, traveling in the caudomedial to craniolateral direction, is a part of the lesser wing of the sphenoid.

Soft tissue structures

The major advantage of CT is that a single set of data can be reconstructed both with a high resolution bone algorithm and with a soft tissue algorithm; this method of reconstruction is better than a simple postprocessing modality, in which window and center line settings are changed. The use of contrast medium is recommended when inflammatory or tumoral changes have to be ruled out. Axial sections are useful in soft tissue settings; image quality of coronal sections can be degraded by dental work. Spiral CT may overcome problems of reformatted images, with an excellent resolution. Reduced acquisition times, and focusing on a stationary object, helps to minimize movement artifacts from the eyes.

The unlimited slice orientation as well as an increased anatomic (T1-weighted) and pathologic (T2-weighted) resolution make MRI superior to CT [2]. In routine studies a head coil provides good image quality of the orbit together with the intracranial structures; for high-resolution examinations a specially designed surface coil is more suitable. MRI examinations should routinely be achieved by T1- and T2-weighted sequences with a slice thickness of 2–4 mm (Fig. 3–5). As in CT the axial slice orientation is recommended primarily, but coronal or sagittal planes along the optic nerve add information about the location and relation of pathologic changes to other structures [3]. Injection of contrast medium (gadolinium-DTPA) injection provides information about the soft tissue perfusion of normal (retina, meningeal sheath of the optic nerve) and pathologic structures. Nowadays the new MRI units offer the advantage of fat suppression techniques to prevent misregistration at the border of fat and water (chemical shift) that may otherwise cause problems in the neighborhood of the optic nerve sheath, the muscles, or the globe [4–7]. Movement artifacts are reduced by short acquisition times; rarely retrobulbar anesthesia may be necessary. Care has to be taken in female patients; cosmetics such as eye shadows or liners may contain metallic material, resulting in major field distortions. An absolute contraindication for MRI studies is foreign metallic material within the globe.

Both CT and MRI are able to delineate the six muscles (four rectus and two oblique) of the orbit, from the cone to the insertion on the sclera. Within the muscle one, the optic nerve travels within the dural sheath

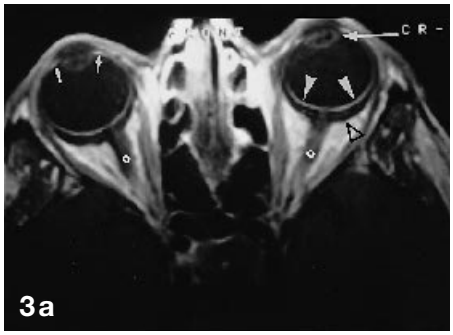

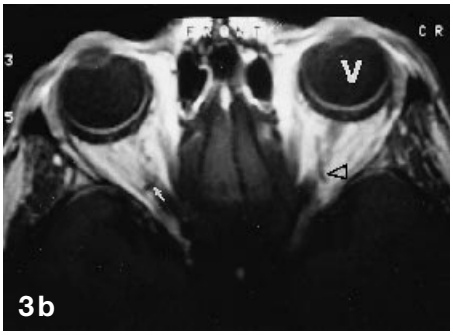

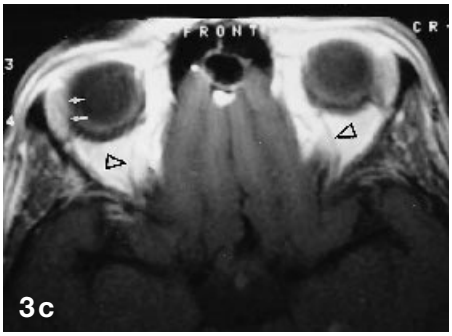

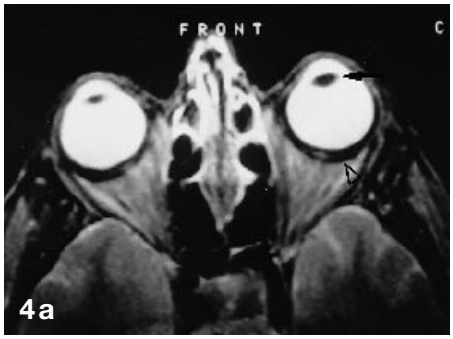

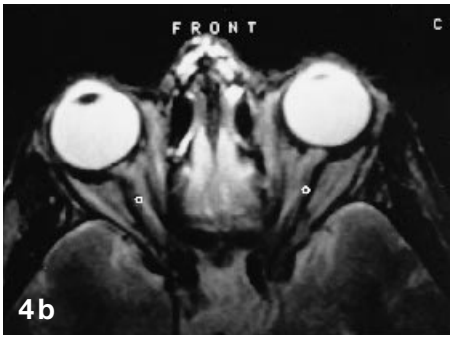

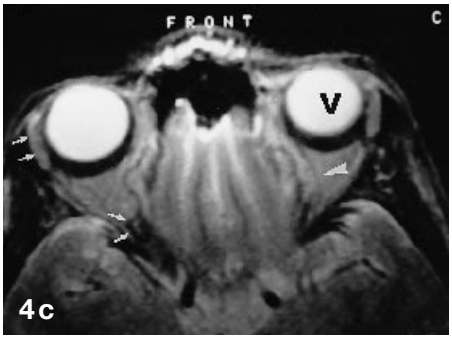

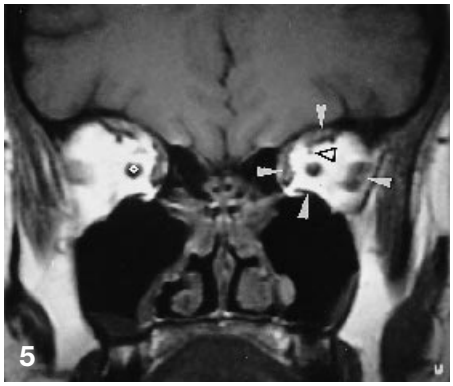

Fig. 3 a, b. Axial MRI scans [slice thickness 3 mm, T1-weighted (T1W) SE sequence]. **a** Mid-section of the lens *(large white arrow).* The ciliary body, iris *(small white arrows),* retina *(white arrowheads),* sclera, Tenon's capsule and chemical shift *(open arrowhead),* and optic nerves *(small circles)* are seen. **b** Globe *(v),* ophthalmic artery *(small white arrow),* and superior ophthalmic vein *(open arrowhead)* are seen. **c** Lacrimal gland *(small white arrows),* and superior ophthalmic vein *(open arrowhead)*

Fig. 4 a, b. Axial MRI scans [slice thickness 3 mm, T2-weighted (T2W) SE sequence]. **a** Good delineation of the globe and the lens *(black arrow),* but major chemical shift *(open arrowhead).* **b** Note the white and black margins of the optic nerves *(small circles)* caused by chemical shift artifacts. **c** Globe *(v),* lacrimal gland *(parallel white arrows),* ophthalmic artery *(small white arrows),* and superior ophthalmic vein *(white arrowhead)*

Fig. 5. Coronal MRI scan (slice thickness 3 mm, T1W SE sequence). There is good delineation of the roof and floor of the orbit. All four rectus muscles *(white arrowheads),* the nerve *(small circle),* and superior ophthalmic vein *(open arrowhead)* are seen

from the posterior pole of the globe via the optic canal to the optic chiasm. Depending on the eye position, the nerve may show a straight or more often serpentine course, which results in a volume-averaging of the proximal third. With the exception of the IInd cranial nerve, the nerve roots entering the orbit through the superior orbital fissure (III, IV, V/1, and VI cranial nerves) are not visible. However, knowledge of their course may give a clue to neurologic deficits. The only important structure of the outer cone is the almond-shaped lacrimal gland, located in the upper lateral aspect of the orbit (Figs. 1 c, 3 c, 4 c).

The globe consists of the retina (innermost layer), the iris, ciliary body, choroid (middle layer), and sclera (outermost layer). Furthermore the globe can be divided into an anterior segment (anterior and posterior chamber) and posterior segment (vitreous chamber). The anterior chamber extends from the cornea to the iris. The posterior chamber is the space between the iris and the lens. The ciliary body is located laterally to the lens and produces aqueous fluid for the anterior segment. The posterior segment or vitreous represents about two-thirds of the globe. Technically CT may show some of the latter structures, but in cooperative patients a high-resolution MRI scan is capable of delineating almost all parts of the globe (Fig. 3 a, b). However, problems may occur in the differentiation between retina, sclera, Tenon's capsule and chemical shift artifacts [7].

Vascular structures

Most of the peripheral orbital vessels are too small to show up on CT or MRI, but when crossing the optic nerve in the posterior third, the ophthalmic artery (90° angle) and superior ophthalmic vein (approx. 20° angle to the optic nerve) are always visualized. Furthermore, the inferior ophthalmic vein is located in a caudal position to the optic nerve and often delineated by MRI. However, DSA is recommended for complete visualization of the arterial and venous system of the orbit [8].

Usually the ophthalmic artery branches immediately from the supraclinoid portion of the internal carotid artery and follows the optic nerve through the canal (sometimes the ophthalmic artery may originate from the middle meningeal artery, or give origin to it). The central retinal artery is the first branch of the ophthalmic artery after it enters the orbit, and courses along the optic nerve to the retina. The next major vessels are the lacrimal artery, and the posterior, as well as the anterior ethmoidal artery. The latter supplies the nasal cavity, parts of the cribriform plate and the anterior falx. The posterior ethmoidal artery supplies the dura, planum sphenoidale and the remaining part of the cribriform plate. In addition to the last major arteries – the supraorbital, supratrochlear and dorsal nasal artery – a number of small muscular branches arise from the ophthalmic artery. Several anastomoses exist between the orbital and maxillary branches [9].

Orbital tumors

Orbital tumors include a large variety of lesions, originating in the optic nerve, the eyeball, and the other soft tissues and bony structures of the orbit. Imaging techniques (mainly CT and MRI) are mandatory for locating and characterizing the lesion, in order to define the optimal treatment. The location in the orbit is important: eyeball (uveal melanoma, and retinoblastoma), optic nerve sheath (meningiomas and gliomas), intraconal (most commonly hemangiomas and neurilemmomas), and extraconal (frequently lymphomas) [10]. In this section, we will focus on optic nerve tumors, vascular lesions, and eyeball abnormalities.

Optic nerve tumors

Before the advent of CT, visualization of the optic nerve was not possible. Secondary signs of optic nerve lesions could sometimes be observed on plain films, mainly widening of the optic foramen, or sclerosis of the sphenoid wings. The introduction of CT, and later MRI, allowed direct demonstration of optic nerve tumors.

Optic nerve sheath meningioma

Meningiomas are benign neoplastic lesions arising from meningoendothelial cells of the meninges. Primary orbital meningiomas, originating in the optic nerve sheath, represent 1–2 % of all meningiomas, and constitute the most common optic nerve tumor after glioma [11]. Orbital meningiomas are more common in females than males (ratio 4 : 1), and they appear most frequently in the fourth and fifth decades of life [12]. Patients typically present with visual loss, frequently associated with optic atrophy; the lesion is usually unilateral, but bilaterality is reported in about 5 % of cases [11]. Clinically, intraorbital optic nerve glioma and meningioma are difficult to differentiate, which highlights the impact of imaging [13].

Typical CT features include either a localized eccentric mass at the orbital apex [14], or a well-defined tubular thickening (64 %), or fusiform swelling (23 %) of the optic nerve [13, 15, 16]. Calcifications are also frequent [12] (Fig. 6). Sclerotic hyperostosis can be observed at the orbital apex, with widening of the optic canal [12, 13]. Moderate to marked enhancement is noted after intravenous contrast injection, occasionally with a central lucent tramline, due to uniform enhancement of a circumferential meningioma (this finding can also be observed in optic neuritis and pseudotumor) [12, 17]. On MRI the meningioma is hypointense to orbital fat on T1-weighted (T1W) images and isointense on T2-weighted (T2W) images, and it shows a mild to marked contrast enhancement after gadolinium-diethylenetriaminepentaacetic acid (Gd-DTPA) [12, 18] (Fig. 7). Fat suppression is useful to separate the enhancing tumor from the orbital fat [12, 19]. MRI is far superior to CT for documenting intracanalicular and intracranial components of the lesion [19]. The intracranial component in optic nerve meningioma is meningeal enhancement, which has a differential diagnostic relevance.

Optic nerve glioma

Gliomas of the optic nerve or visual pathway are benign astrocytic neoplasms that primarily affect children in the first decade of life [12, 20]. The lesion can involve various portions of the optic retrobulbar pathways, including the optic nerve, chiasm, optic tracts, and radiations. The tumor shows early growth, followed by stability in many patients; if the lesion is initially confined to the optic nerve alone, overall mortality is low (5 %), whereas it rises to about 50 % in cases of involvement of the hypothalamus [21]. Optic nerve gliomas are more frequent than meningiomas (ratio 4 : 1) [22, 23]. There is no significant sex prevalence. Approximately 15 % of patients with optic nerve gliomas exhibit findings of neurofibromatosis type-1 (NF) at the time of diagnosis [13, 24]; when glioma is bilateral, NF should be strongly suspected.

Malignant optic glioma is a distinct disease, which occurs in middleaged adults [21, 22]. The clinical presentation depends on the location of the tumor; in cases of intraorbital optic nerve glioma, there is usually painless proptosis, and optic atrophy is also frequent [12].

CT features include moderate to marked diffuse swelling of one or both nerves, with frequent kinking or buckling of the enlarged nerve; moderate to intense enhancement is observed after contrast injection, frequently with internal lucencies [13, 25] (Fig. 8 a). Extension through the optic foramen causes widening of the optic canal. Precise anatomic definition of the tumor is better on MRI than CT, mainly when the glioma passes through the optic canal [13, 26]. The lesion is hypointense to orbital fat on T1W images, and mixed to homogeneous and hyperintense on T2W images [13, 27] (Fig. 8 b, c); contrast enhancement is usually evident [13].

Other tumors of the optic nerve are rare. They include hemangioblastoma, hemangiopericytoma, choris-

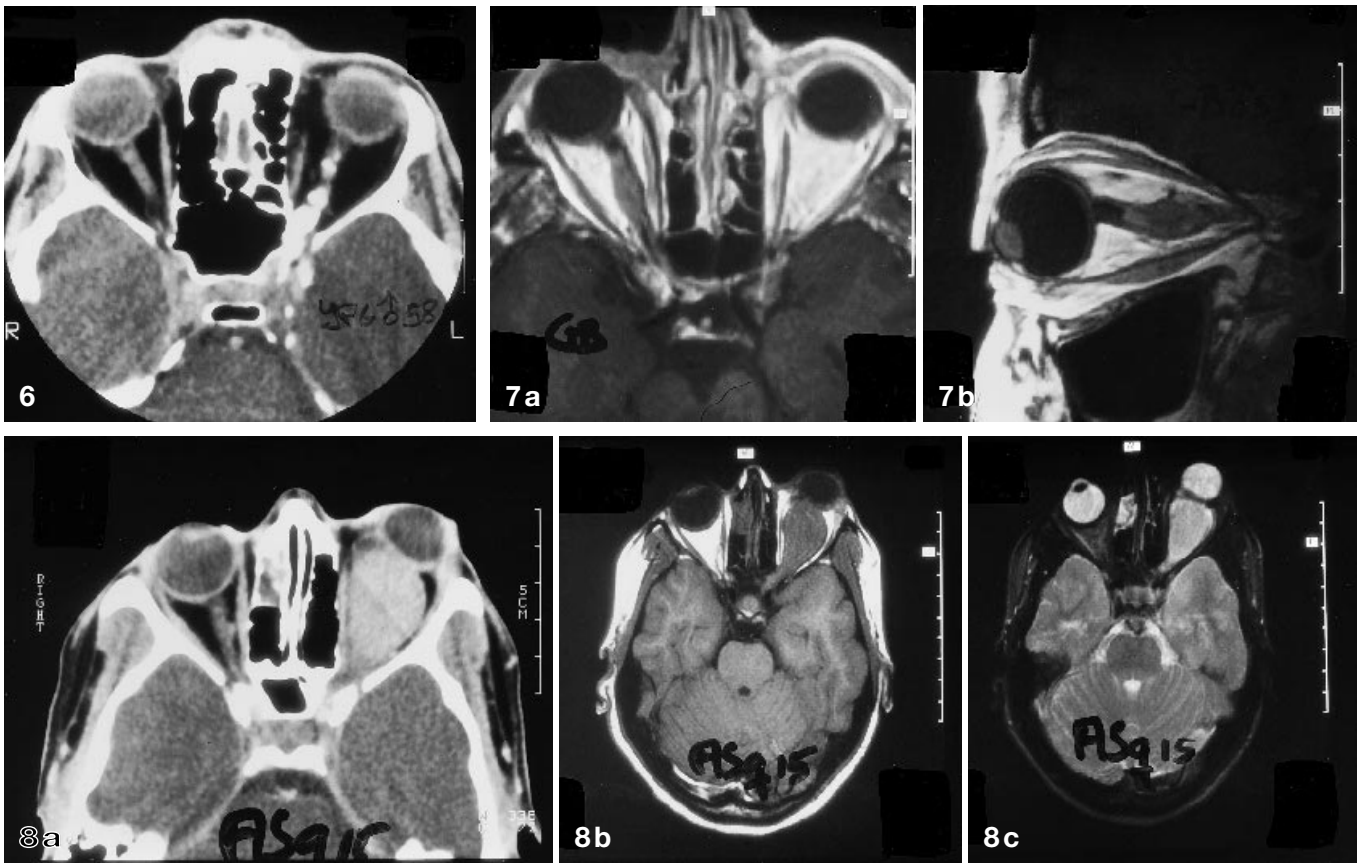

Fig. 6. Left optic nerve sheath meningioma in a 58-year-old man; contrast-enhanced axial CT scan. Note calcifications extending through the optic canal

Fig. 7 a, b. Right optic nerve sheath meningioma in a 53-year-old man; MRI scan after Gd-DTPA. **a** Axial and **b** sagittal views. Observe swelling of the nerve, with contrast enhancement

Fig. 8 a–c. Left optic glioma in a 15-year-old girl. **a** Enhanced axial CT section, **b** unenhanced T1W, and **c** T2W MRI sections. Observe the significant fusiform swelling of the nerve, hypointense to orbital fat on T1W, and hyperintense on T2W images

toma (which is a rare benign tumor, containing fat and smooth muscle [28]), metastasis, and extension to the nerve of an intraocular tumor (melanoma and retinoblastoma). Nontumoral enlargement of the optic nerve is also observed in many other conditions. Briefly it can occur in systemic diseases such as sarcoidosis, toxoplasmosis, tuberculosis and syphilis, in optic neuritis, in trauma, in pseudotumor and Graves' disease, and also in cases of increased intracranial pressure [12, 13, 29].

Vascular abnormalities

Capillary hemangioma

Capillary hemangiomas occur in infants during the first year of life. The size increases for 6–10 months, and then involution is observed [25]. The lesion is frequently extraconal, usually in the superior nasal quadrant [12]. Arterial supply is pronounced, from the external and/or internal carotid artery, with risks of significant bleeding [12, 25]. On CT the lesion is ordinarily well delineated, and sometimes ill defined; it enhances significantly and homogeneously [12]. On MRI, hypo- or slight hyperintensity is observed on T1W images, hyperintensity on T2W images, and there is intense contrast enhancement [12] (Fig. 9).

Cavernous hemangioma

Orbital cavernous hemangioma is the most common orbital vascular tumor in adults [12, 25]. It occurs anywhere in the orbit, most frequently in the retrobulbar muscle cone. The tumor is slowly progressive, and does not spontaneously involute. As there is usually a fibrous pseudocapsule, surgical excision is easy, without fragmentation [25]. On CT, the lesion is well delineated, smooth and homogeneous, with variable contrast uptake (Fig. 10); on MRI the lesion is iso- to slightly hyperintense on T1W images, significantly hyperintense on T2W images, and enhancement is variable [12].

Orbital lymphangioma

Orbital lymphangioma occurs in children and young adults, and is most frequently extraconal. The lesion is slowly progressive, without spontaneous regression [25]. Due to absence of a capsule, infiltrative features

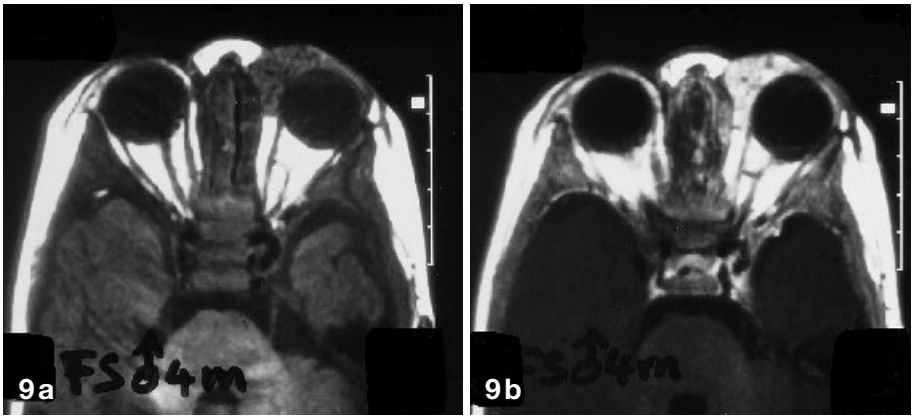

Fig. 9 a, b. Left capillary hemangioma in a 4-month-old boy; axial MRI sections before (**a**), and after (**b**) intravenous Gd-DTPA. The fairly well delineated lesion is typically located in the upper nasal quadrant, and is isointense on the T1W image, with marked contrast uptake

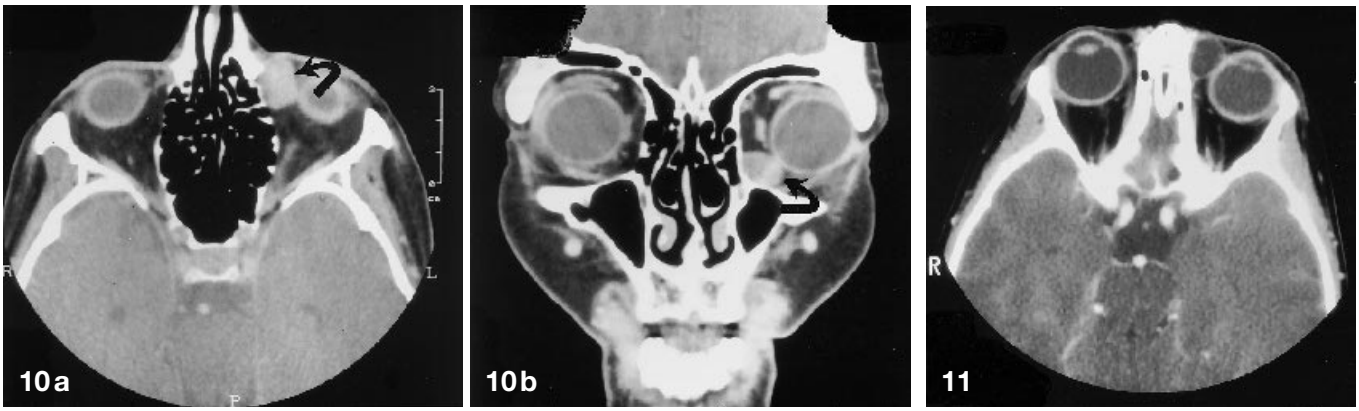

Fig. 10 a, b. Left cavernous hemangioma in a 63-year-old woman, presenting with painless swelling of the left internal canthus, contrast-enhanced axial (**a**) and coronal (**b**) CT sections. The lesion *(curved arrow)* is fairly well delineated, and shows significant homogeneous enhancement; the eyeball is pushed slightly laterally. Note the discrete bone remodeling of the left anterior-inferior lamina papyracea, without bone erosion

Fig. 11. Left dermoid cyst; contrasted-enhanced CT section. The cyst is hypodense, with a thin enhancing rim

are typical, with subsequent difficulty in surgical resection. Intratumoral haemorrhages are frequent, which cause increased proptosis [25]. On CT the lesion is spontaneously hyperdense and heterogeneous, with little, or sometimes marked enhancement. Usually it is poorly delineated (which allows differential diagnosis with hemangioma). On MRI the lesion is hyperintense on T1W images, and mainly on T2W images [12, 25].

Dermoid and epidermoid cysts

Dermoid and epidermoid cysts result from inclusion of ectodermal elements during closure of the neural tube [12]. Cysts usually develop along the superotemporal orbital rim and are often attached to the orbital bones due to dermal elements pinched off along suture lines [30]. On CT the lesion is smoothly marginated and well delineated, with a large and hypodense center; rim enhancement is observed and calcifications may be seen [12] (Fig. 11). On MRI the lesion is hyperintense on T1W images and heterogeneous on T2W images. Ruptured dermoid cysts have a different signal, and may be mistaken for hemangiomas.

Eyeball tumors

Retinoblastoma

Retinoblastomas are highly malignant tumors, arising from neuroectodermal cells (nuclear layer of the retina). They are of congenital origin, but not recognized at birth. Ninety percent of lesions are detected in young children below 5 years of age, and bilaterality is observed in approximately 30 % of cases [12, 31]. The diagnosis should be setted quickly, as, with limited disease, the 5-year survival rate is excellent (92 %), and useful vision of the treated eye can be maintained in most patients, whereas in cases of extension beyond the eye there is 100 % mortality [12, 32, 33].

The role of CT and MRI is first to reveal whether there is retrobulbar extension, intracranial metastasis, or a second tumor, and to differentiate retinoblastoma from simulating lesions (persistent hyperplastic primary vitreous, Coats' disease, retinopathy of prematurity, toxocariasis, retinal detachment, and many other conditions) [12].

CT features include calcifications in more than 90 % of cases, which can be single or multiple [12, 34] (Fig. 12). It should be stressed that CT demonstration of intraocular calcification in a child less than 3 years old represents retinoblastoma [12]. The tumor shows

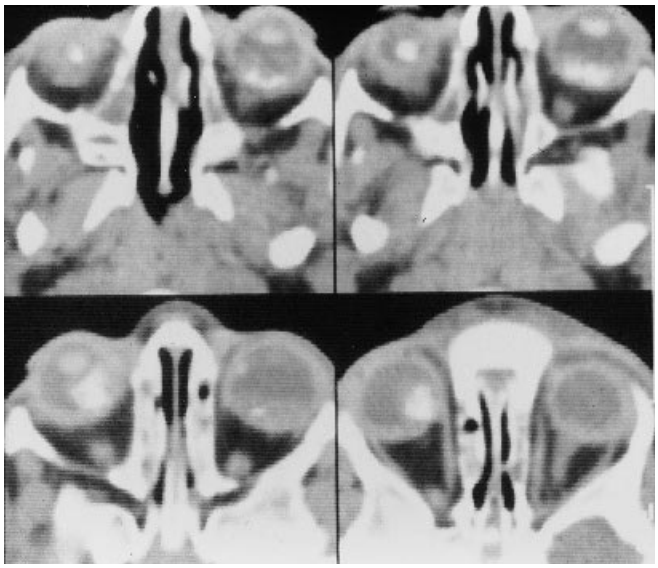

Fig. 12. Bilateral retinoblastoma in a 2-year-old boy; contrast-enhanced axial CT views. Note extensive calcifications in both eyeballs, irregular swelling of the posterior wall of the right eye, and subretinal fluid on the left

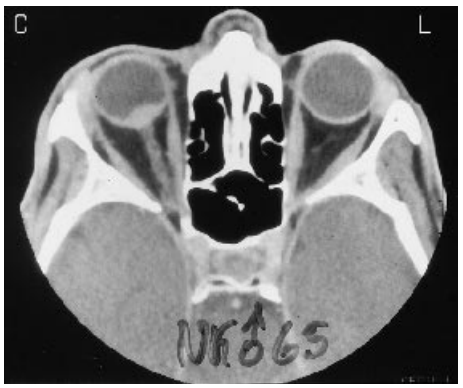

Fig. 13. Right uveal melanoma in a 65-year-old man; contrast-enhanced CT scan. The enhancing lesion covers the optic disk, without visible infiltration of the nerve

moderate contrast enhancement. MRI is not as specific as CT for diagnosing retinoblastoma, due to its lack of sensitivity in detecting calcifications [12], but MRI differentiation from simulating lesions is possible. The tumor is slightly hyperintense to the vitreous on T1W images, and significantly hypointense on T2W images [12]. MRI is better than CT for visualizing the optic nerve, and intracranial involvement [12].

Malignant uveal melanoma

The uveal tract is highly vascular. Malignant melanomas exhibit various cell types, with a varied prognosis. Associated subretinal fluid is frequent. There is an excellent 5-year survival rate when the diagnosis is made on a lesion less than 10 mm in diameter and 3 mm thick [35]. Sometimes the lesion can be stable. Usually the diagnosis is made by ophthalmoscopy, fluorescein angiography and ultrasonography. CT and MRI evaluate the extent of the lesion, and are also useful in cases of opaque media. Melanomas are usually elevated and sharply defined, with spontaneous hyperdensity on CT (Fig. 13) and, on MRI, if melanotic, hyperintensity to the vitreous on T1W images and hypointensity on T2W images [12]. MRI is now the gold standard, particularly as it allows differentiation of the lesion from associated subretinal exudate, which is usually not possible by CT.

Other orbital masses

Other orbital masses include metastasis, lymphoma (lymphoid tumors represent 10–15 % or orbital masses, and are frequently localized in the anterior orbit [12]), and lacrimal gland tumors.

Angiography

Diagnostic angiography

Selective catheterization of the internal carotid artery (ICA) is normally done via puncture of the femoral artery. An approach via the axillary artery or brachial artery is chosen only if the femoral artery is occluded. A 5 Fr diagnostic catheter is recommended because it significantly reduces the risk of vasospasm and thromboembolism in comparison with larger catheters. In selective and superselective angiography the contrast medium is applied manually to minimize trauma to the vessel wall, and to be able to stop injection in case of clinical or angiographic conspicuity.

In cases of orbital pathology the diagnostic angiography must demonstrate the arterial system of the ICA and external carotid artery (ECA), particularly the arterial supply to the orbit, and the possibility of dangerous branches or anastomoses, especially of the ECA. Every angiographic study should include at least two different views of a vessel, usually the posteroanterior and lateral projections. Selective and often even superselective injections should be performed and a protocol of angiographic exploration designed for each case. In addition, the angiographic investigation should include determination of the intracranial collateral circulation at the level of the circle of Willis in every lesion with a relationship to the ICA.

Topographic information concerning a tumor of the orbit is more precisely given by MRI and CT. The main indications for angiographic examination of the orbit are vascular changes such as carotid-cavernous fistula (spontaneous or post-traumatic), aneurysms, angiomas, Rendu-Osler disease, and congenital syndromes (e. g., Wyburn-Mason syndrome). In most cases angiography is done not because of diagnostic problems, but for ascertaining the possibility of an interventional procedure. Exploring the possibility of intervention is equally or more important in cases of tumoral lesions originating within the orbit such as gliomas, lymphomas, hemangi-

omas, and optic nerve meningiomas, and for tumors invading from the periphery such as meningiomas, and metastases from the skull base, esthesioneuroblastoma, adenocarcinoma or squamous cell carcinoma from the nasosinus cavities, and angiofibroma arising from the nasopharynx. For differential diagnosis of orbital tumors angiography is only very rarely necessary.

Therapeutic angiography: general considerations

Digital subtraction angiography (DSA) is mandatory when performing neuroradiologic embolization procedures. It provides excellent image quality and shortens the procedure time by producing instantaneously subtracted images. DSA has a higher contrast resolution than conventional film angiography, without significant loss of spatial resolution, and it additionally allows the use of reduced amounts of diluted iodinated contrast agent.

The procedure can be performed with the patient under general or local anesthesia. General anesthesia guarantees optimal working conditions for the interventional neuroradiologist. The introduction of highly flexible microcatheters has significantly reduced the incidence of spasm in the ECA territory. Therefore increasing numbers of embolizations are now performed under local anesthesia. Permanent balloon occlusion of the ICA requires local anesthesia because active cooperation of the patient is mandatory.

Neuroradiologists performing endovascular therapy must be familiar with the vascular anatomy of the orbit, and the dependence of clinical symptoms on vascular territories [36–42]. Only this knowledge allows adequate patient selection with precise definition of therapeutic goals, thereby avoiding dangerous complications, and improving the reliability and safety of endovascular therapeutic procedures. The radiologist must also be familiar with catheter techniques and the different embolic materials, because, from the technical point of view, catheterization selectivity and the embolic material determine the success of embolization [36, 43–46].

The continuing development of microcatheters and microguidewires has enabled the superselective catheterization and embolization of the petrous and cavernous branches supplying the ICA, and of the ophthalmic artery. The relationship of the inner diameter of the vessel to the outer diameter of the catheter and its geometry limit the distance within a small artery that can be reached in catheterization. For example, there is currently no possibility of reaching the central retinal artery selectively.

The choice of embolic material depends on the goal of the procedure, the selectivity to be accomplished, and the vascular anatomy of the pathologic territory [45–48]. As a general rule, microparticles are preferable to fluid materials in preoperative tumor embolization because they are easier and safer to use, and, if properly sized, can reach the intratumoral microvasculature. Detachable balloons are the agent of choice for most cases of direct single-hole arteriovenous fistula, or for carotid artery occlusion.

Since embolization of orbital tumors is nearly always a preoperative measure followed by surgical removal, every effort should be made to minimize morbidity. The most serious complications associated with interventional procedures include cerebral stroke, blindness, and cranial nerve palsies. The main reasons for such complications are lack of knowledge concerning the vascular anatomy of the ECA, and the reflux of embolic material into physiologic vessels supplying normal tissue [36, 38, 39, 41, 48].

Therapeutic angiography: interventional procedures

Vascular intervention in the region of the orbit can be divided into two opposing procedures: the re-canalization (opening) of occluded vessels, and the embolization (closing) of pathologic vessels, mostly caused by tumor or traumatic changes.

Re-canalization procedures

Only one re-canalization procedure is of importance for the orbit. This is local intra-arterial fibrinolysis (LIF), which is done mainly in cases of acute thromboembolic occlusion of the ophthalmic artery [9, 49]. To perform LIF, a microcatheter is placed in the proximal part of the ophthalmic artery, and approximately 1 million units of urokinase or 20 mg recombinant tissue-type plasminogen activator (r-TPA) administered within 2 h. This procedure is still under discussion, and further investigations are necessary. Concerning the treatment of thrombosis of the central retinal vein, there is even less proven therapy. Some groups have tried systemic thrombolysis, while others do not treat actively at all. LIF in the case of occlusion of the vein is only mentioned anecdotally within the ophthalmologic literature.

Occluding procedures

The only curative occluding procedures within the region of the orbit are those for the treatment of aneurysms and arteriovenous fistulas, by permanent *balloon occlusion* [41, 43]. A carotid-cavernous sinus fistula represents an acquired intracranial arteriovenous shunt between the carotid artery and the cavernous sinus. Clinical findings are pulsating exophthalmos, pulsosynchronous intracranial bruit, palsy of cranial nerves III, IV and VI, and chemosis of the eye. Accompanying acute subarachnoid or intracranial hemorrhage has also been reported. These fistulas are usually caused through major facial or craniocerebral trauma. The trauma may be blunt, with or without skull base fractures, or it may be penetrating from the orbit to the intracranial space. Angiographic evidence consists of early and dense opacification of the cavernous sinus, early filling of its drain-

ing veins, especially the superior ophthalmic vein, and poor opacification of cerebral vessels. It is important to perform angiography of the ICA and ECA, both left and right, and of the vertebrobasilar system. The pulsating exophthalmos may develop unilaterally (ispsilateral or contralateral) or bilaterally, depending on the venous outflow of the cavernous sinus. Bilateral carotid-cavernous fistulas may also occur. Often there is a delay between the traumatic event and the clinical manifestation.

Although the fistula is usually supplied through a tear in the ICA, it may, occasionally receive blood from branches of the ICA or ECA, or from the vertebrobasilar system, via the posterior communicating artery. Venous drainage is primarily into the superior ophthalmic vein, but may also extend into various venous outflows, including the contralateral cavernous sinus, the inferior ophthalmic vein, the pterygoid plexus, the sylvian veins, and the petrosal sinuses.

Nonsurgical, endovascular treatment is the method of choice for closure of the fistula, which can be performed utilizing detachable balloons, or coils delivered into the cavernous sinus. Reconstructive embolization with preservation of the patent ICA can be achieved in most cases. If this is not feasible, the carotid artery may be occluded nonsurgically above and below the fistula, using detachable balloons.

If reconstructive embolization appears to be possible, an endoarterial route is taken for the catheter, with occlusion of the fistula by inflating a detachable balloon on the venous side. In these lesions, endovascular embolization is the treatment of choice, because it has a cure rate of 95 %, entails very little risk, and produces significantly less morbidity and hospitalization than any other form of treatment. Detachable balloons can usually be placed directly at the site of the abnormal arteriovenous communication, with little or no traumatic disturbance to other tissues or organs (Fig. 14). Another route is the venous approach, either via the petrosal sinuses, or by cannulating the widened superior ophthalmic vein [50], in cooperation with an ophthalmologist.

Besides the traumatic one-hole fistula, there is a second type of dural carotid-cavernous fistula which mainly develops in elderly women. However, these often numerous small fistulas between extradural branches and the sinus often elude complete cure via interventional procedures.

Permanent balloon occlusion of the ICA is a frequently performed procedure for aneurysms of the distal ICA, and for skull base vascular injuries [43] that are secondary to trauma, or (less frequently) iatrogenic. In these cases the vessel is often so badly damaged that a reconstructive embolization is impossible, and the artery has to be sacrificed by trapping the fistula. Rarely the ophthalmic artery has to be occluded in cases of tumorous or vascular lesions. Fortunately in 90 % of cases collateral blood supply is adequate after occlusion of the ICA or the ophthalmic artery. As long as the occlusion of the ICA is inferior to the ophthalmic artery, collateral supply is possible via the circle of Willis. When the ophthalmic artery itself must be occluded, collaterals from branches of the ECA can often secure the blood supply.

Embolization of lesions of the orbit is mainly performed for vascular tumors supplied by branches of the ECA and/or the ICA. It represents a purely preoperative measure; it is not able to cure neoplasms, because the embolization only treats the vascular component of the tumor. Such tumors may be meningiomas, squamous cell carcinomas or adenocarcinomas, metastases, or angiofibromas. Any preoperative embolization of vessels with particles or fibrin glue is temporary, and because of new collaterals and/or recanalization tumor surgery should be done within a maximum of 5 days. The goal of preoperative devascularization of vascular neoplasms is selective obliteration of the pathologic intratumoral vasculature, while preserving the normal supply to surrounding tissues. Obliteration with appropriate embolic materials facilitates the subsequent surgery. For patients in a poor general clinical condition, in whom prolonged anesthesia is not possible, and for patients who refuse surgery, embolization can be performed as a palliative measure. Incurable malignant tumors and/or osseous metastases from strongly vascularized tumors, such as thyroid carcinoma, or hypernephroma, may be extremely painful, and refractory to analgesic drugs. In most cases embolization reduces the pain significantly, with immediate symptomatic relief. Furthermore, it may reduce the space-occupying changes, such as proptosis caused by tumor growth.

Meningiomas represent one of the most important indications for preoperative embolization of skull base lesions, because of their frequency and their hypervascularity [9, 48, 50]. The obligatory meningeal arterial supply of meningiomas typically arises from the dural base of the tumor. Meningiomas exhibit a characteristic angiographic appearance consisting of dilated meningeal feeding arteries, converging towards the dural site of the tumor, radiating intratumoral dural arteries, and a more or less homogeneous blush of variable intensity, usually persisting into the late venous phase.

Frontobasal meningiomas include meningiomas of the orbital roof, the olfactory groove, and the planum sphenoidale. Because of the rather small size of the supplying dural branches, the unfavorable vessel geometry, and the dangers associated with the ophthalmic artery territory, the role of embolization in frontobasal meningiomas is rather limited. Meningiomas of the sphenoid wing and middle cranial fossa receive their dural supply from the sphenoidal branch and the middle cranial fossa branches of the middle meningeal artery respectively. Meningiomas of the cavernous sinus and perisellar area receive their supply from multiple dural arterial sources, the most frequently observed being the inferolateral trunk arising from the lateral wall of the C4 portion of the ICA, and anastomosing with the accessory meningeal artery, the lateral clival artery arising from the C5 portion of the ICA, the cavernous branch of the middle meningeal artery, and the recurrent meningeal branch of the ophthalmic artery. Meningiomas in this area reveal a close relationship with the ICA. Permanent preoperative balloon occlusion of the ICA should be con-

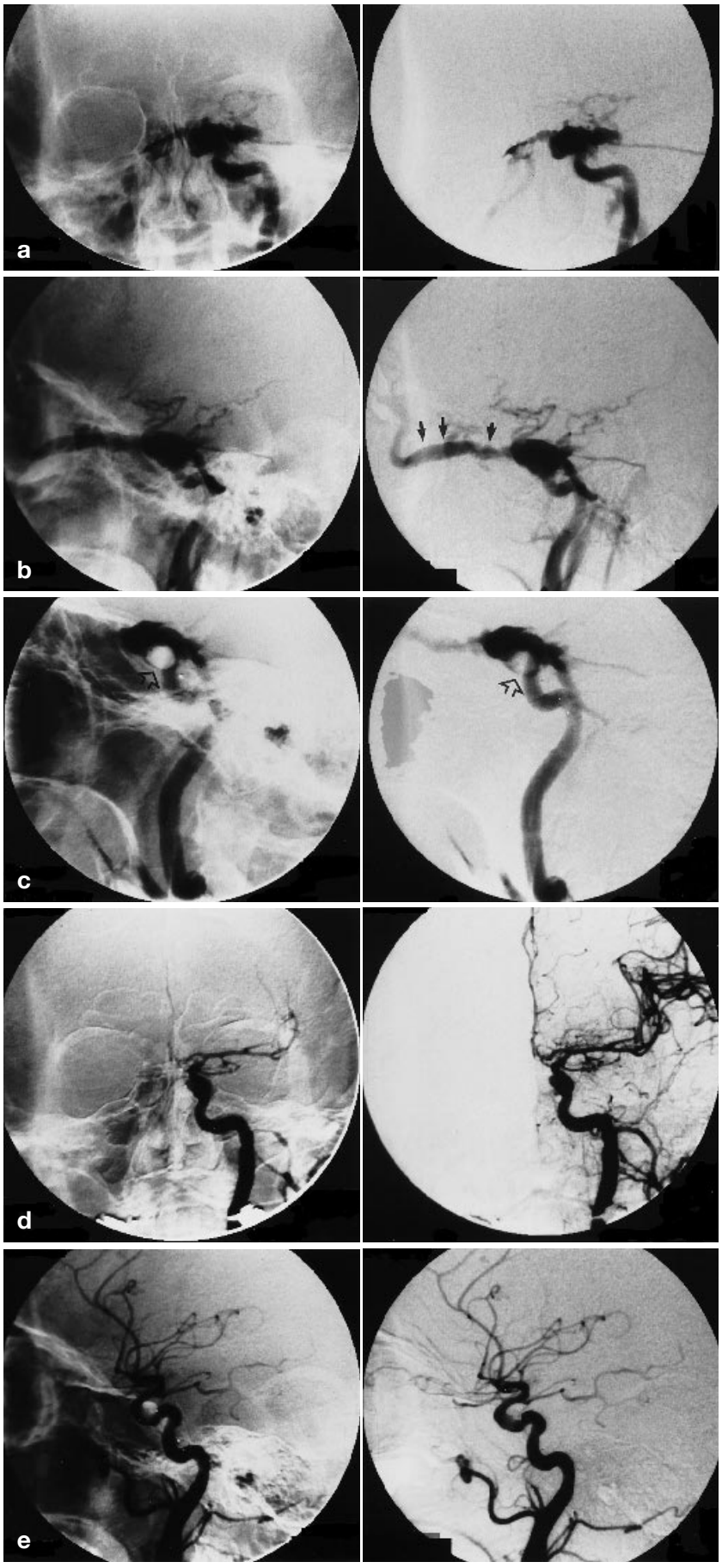

Fig. 14a–e. Skull trauma and left-sided exophthalmos in a 50-year-old man. Selective angiography (*left:* bone window, *right:* soft tissue window) showed in both planes (**a, b**) a typical carotid-cavernous fistula (CCF) with a dilated ophthalmic vein *(arrows)* and venous drainage of contrast material within the early arterial phase. **c** Placement of the balloon *(open arrow)* via the endoarterial route and partial reduction of flow within the fistula. **d, e** After detachment of the balloon, there was closure of the CCF with a preserved and patent internal carotid artery in both planes

sidered if selective angiography demonstrates irregular narrowing of the vessel lumen.

The great majority of juvenile nasopharyngeal angiofibromas (JNA) develop in young males around puberty. This histologically benign, fibrovascular tumor with the potential for locally aggressive behavior becomes symptomatic by nasal obstruction, and variable degrees of epistaxis. Radical surgical tumor removal after preoperative embolization is the treatment of choice [9, 37, 40, 42, 44, 51, 52]. Angiographically, this tumor has a nearly pathognomonic appearance, because, in contrast to most other tumors of this region, the supplying arteries arising from the ECA and ICA are only minimally dilated. The intense tumor blush appears during the arterial phase, and persists until the late venous phase. The contralateral ECA often participates in such JNAs, which reach or extend over the midline, and has to be examined in these cases. The first and constant arterial system supplying this kind of tumor is seen in the nasopharyngeal and nasal cavity branches of the internal maxillary artery. The accessory meningeal, the ascending pharyngeal, and the descending palatine arteries may participate in case of larger tumor extension.

In Rendu-Osler disease, selective embolization of the involved vessels may reduce the risk of bleeding. The most frequently involved vessels are arteries of the face and nose, but sometimes there is also involvement of branches of the ophthalmic artery (often following surgical occlusion of the maxillary artery). However, neuroradiologic intervention is here again of only temporary use, this time not due to recanalization but because of the natural course of this progressive disease. A rare case and even more rare treatment of an intracranial arteriovenous malformation with extracranial and retinal malformation (Wyburn-Mason syndrome) has been reported with interventional occlusion of the feeding vessel [46].

Orbital inflammation

Orbital inflammation includes infection (usually a complication of sinusitis), foreign bodies and trauma, pseudotumor, thyroid orbitopathy and optic neuritis.

Bacterial orbital infection

Most cases of orbital cellulitis are due to sinusitis. The patient presents with ocular pain, lid edema, chemosis, proptosis, limited eye mobility, fever, and elevated white blood cell count. If prompt treatment is not instituted, serious complications occur, with blindness, cavernous sinus thrombosis, and epidural, subdural, and brain abscesses [12, 53]. Classification of orbital cellulitis includes five stages: (a) preseptal inflammation (eyelid edema or abscess), (b) subperiosteal inflammation (phlegmon and abscess), (c) orbital cellulitis, (d) orbital abscess, and (e) venous thrombosis (ophthalmic vein and cavernous sinus) [12, 30]. Imaging (mainly CT) is very useful in acute settings to differentiate subperiosteal phlegmon (heterogeneous swelling, with muscle displacement), which is usually treated conservatively, from subperiosteal abscess (pus collection in the subperiosteal space) (Fig. 15), which necessitates surgery.

Orbital complications of endoscopic sinus surgery are of diagnostic importance, and fairly frequent. Minor complications occur in 5 % of cases, following surgical violation of the lamina papyracea; they include hematoma and edema of the internal canthus and inferior eyelid, or orbital emphysema. Major complications are rare, with diplopia following surgical lesions of the extrinsic muscles, blindness (either directly iatrogenic, or due to ischemia of the nerve by compressive hematoma), and orbital abscess [54].

Foreign bodies of the eyes and orbit

Foreign bodies (FB) represent ophthalmic emergencies, and require thorough evaluation to define appropriate treatment. In most ocular trauma, it is mandatory to look for, and eventually localize, a foreign body. Ophthalmoscopic examination is usually difficult, due to opacified cornea and opaque media. Complications of FB include hemorrhage, traumatic cataract, infection, and also chemical damages. The majority of FB lie on the surface of the cornea, conjunctiva, or anterior sclera, and are thus easily removed. When metallic, the FB are intraocular, or retrobulbar. Orbital FB are not removed, unless interference with mobility or injections occur.

Conventional films are effective for most intraocular metallic FB (larger than 1 mm). CT is useful for smaller metallic FB and nonmetallic FB (Fig. 16 a). In cases of wooden FB, fresh wood is usually hyperdense, on CT, whereas dry wood is hypodense sometimes indistinguishable from orbital fat, or intraorbital air [55, 56]. MRI can be useful to differentiate FB (hypointense) and orbital fat [56]. Glass FB are hyperdense, but without the typical streak artifacts that are observed in metallic FB (Fig. 16 b). Finally, MRI is usually contraindicated in cases of proven or suspected intraocular metallic FB.

Orbital pseudotumor

Inflammatory orbital pseudotumor is a term used to describe any idiopathic inflammatory lesion of orbital tissue that simulates a neoplasm of the orbit; it is a definite clinical entity with various forms, covering a wide spectrum of periocular lesions [57, 58]. This syndrome has been confused for many decades with thyroid orbitopathy, and lymphoid tumors. It can occur at any age; in children it is frequently bilateral, whereas bilaterality is less common in adults. Exophthalmos, pain and inflammation are usually observed in acute stages. Usually the prognosis is good with steroid therapy. The spectrum of orbital pseudotumors includes anterior inflammation, diffuse orbital inflammation, myositic abnormality, apical lesions, lacrimal adenitis, and perineuritis [12].

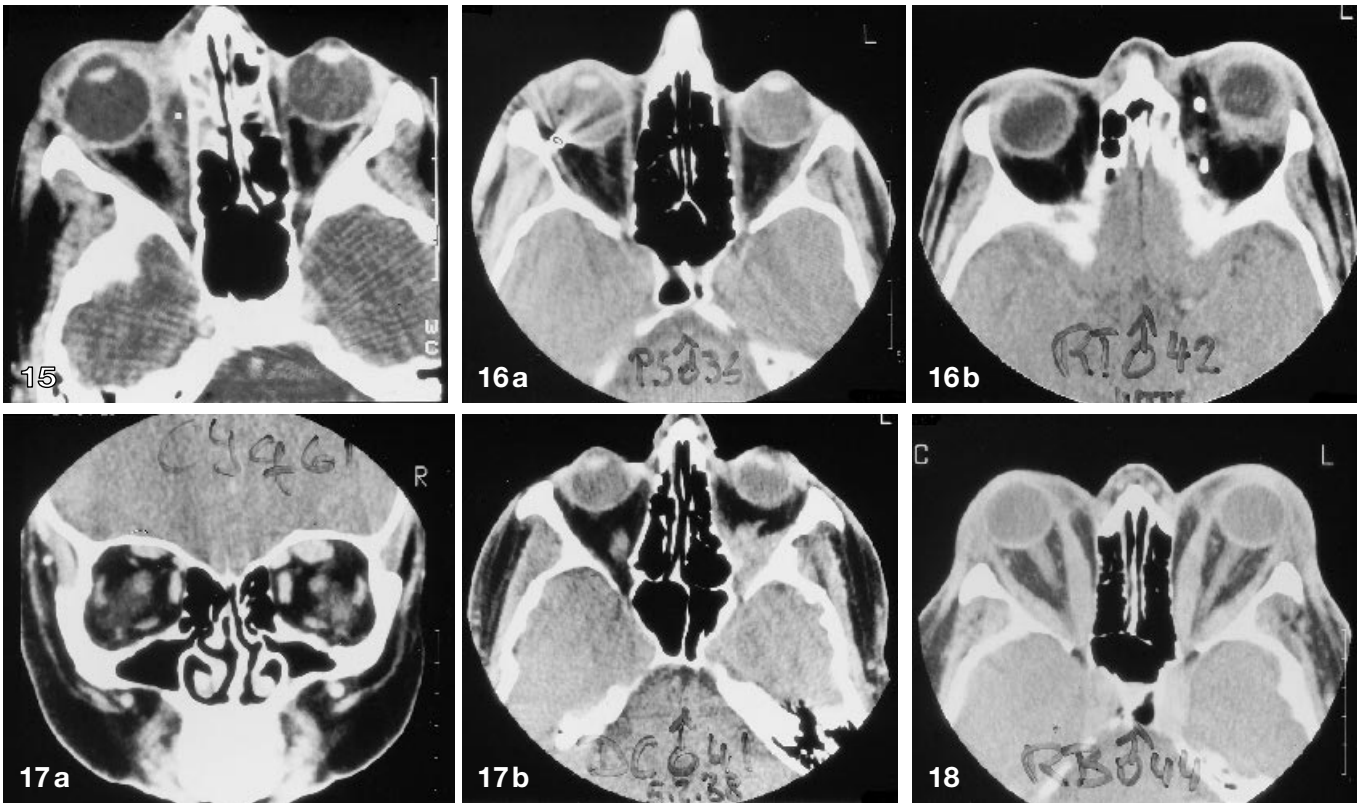

Fig. 15. Orbital subperiosteal abcess; contrast-enhanced CT section. Note the slight proptosis of the right eye, inflammatory disease of the right anterior ethmoid cells, with subperiosteal abcess *(white square),* and lateral displacement of the medial rectus muscle

Fig. 16 a, b. Orbital foreign bodies (FB); axial CT sections. **a** Right metallic FB in a retrobulbar position; observe the significant streak artifacts, and a small post-traumatic bubble of air in the vitreous. **b** Glass FB in the left orbit; despite marked hyperdensity, the absence of streak artifacts allows differentiation from a metallic FB

Fig. 17 a, b. Orbital pseudotumor in two different patients. **a** Contrast-enhanced coronal CT scan in a 61-year-old woman; observe the muscle swelling involving mainly the upper group, and to a lesser extent the medial rectus, and the trochlear muscles. **b** Contrast-enhanced axial CT scan in a 41-year-old man; note the marked infiltration of the left orbital apex, without bone destruction

Fig. 18. Graves' orbitopathy in a 44-year-old man; contrast-enhanced axial CT section. Note the symmetric bilateral abnormalities, with significant proptosis, and moderate swelling of the extraocular muscles. The orbital fat is also slightly infiltrated

Of the various CT features associated with the different forms of pseudotumor, the most frequent include enhancement after intravenous contrast injection (95 %), infiltration of the retrobulbar fat (76 %), proptosis (71 %), extraocular muscle enlargement (57 %), apical fat infiltration and edema (48 %), muscle tendon or sheath enlargement (43 %), and optic nerve thickening (38 %) [59] (Fig. 17). In cases of muscle enlargement, the superior complex and medial rectus are most frequently affected. The muscle borders are a little ragged, and fluffy [12]. These features allow differentiation from Graves' orbitopathy. A key finding is the absence of bone erosion or remodeling, which are common in benign and malignant tumors [12, 59].

Thyroid orbitopathy

Thyroid (or Graves') orbitopathy usually affects middle-aged women, and is due to an autoimmune process. Painless proptosis is commonly noted, with gradual diplopia, and is frequently bilateral [12]. Radiologic examination of patients with Graves' disease is routinely done with CT [60–62]. Typically CT discloses enlargement of the extraocular muscles (Fig. 18); the most frequent pattern of muscle involvement affects all muscles [60]. When an isolated muscle is involved, the inferior rectus is most commonly affected [12]; however, some authors report the superior muscle to be involved most frequently [60]. The muscle belly is enlarged, sometimes significantly, with well-defined borders, and its tendon is preserved; these features allow differentiation from pseudotumor. The intraorbital fat is increased, and usually homogeneous, and proptosis can be significant. Enlargement of the retrobulbar optic nerve sheath and of the superior ophthalmic vein are also common. MRI can be useful in Graves' disease to evaluate the muscle changes (edema, fibrosis, and fatty degeneration), in order to allow standardized planning of therapy, and follow-up [63]. Furthermore, MRI is more suitable than CT in cases of significant muscle enlargement, with optic nerve crowding at the orbital apex and subsequent optic neuropathy, in order to evaluate the degree of fat effacement, which is a measure of optic nerve compression [64].

Optic neuritis

Optic neuritis is an acute inflammation of the optic nerve, which is frequently enlarged. In many cases it is the early manifestation of multiple sclerosis. On CT, the enlarged nerve shows moderate contrast uptake, and on MRI it is hyperintense on T2W images [12].

References

1. Mohr C, Seifert V, Stolke D, Sievers K, Schettler D (1994) Planning of anterior skull base reconstruction aided by presurgically computer-generated models. In: Samii M (ed) First international skull base congress. Karger, Basel, pp 609–612
2. Sievers KW, Wegener-Panzer A (1994) Die Computer- (CT) und Magnetresonanztomographie (MRT) in der orbitalen Diagnostik. In: Lund O-E, Waubke TN (eds) Bildgebende Verfahren in der Augenheilkunde. (Bücherei des Augenarztes, vol 133) Enke, Stuttgart, pp 10–20
3. Wegener-Panzer A (1995) The orbit. In: Löhr E, Sievers KW, Faiss J, Diener HC, Stolke D (eds) Clinical neuroradiology. Huber, Bern, pp 27–38
4. Dixon WT (1984) Simple proton spectroscopic imaging. Radiology 153: 189–194
5. Keller PJ, Hunter WW Jr, Schmalbrock P (1987) Multisection fat-water imaging with chemical shift selective presaturation. Radiology 164: 539–541
6. Simon J, Szumowski J, Totterman S, Kido D, Ekholm S, Wicks A, Plewes D (1988) Fat suppression MR imaging of the orbit. AJNR 9: 961–968
7. Sievers KW, Dietrich U, Löhr E (1991) Über Phasen-, Frequenz- und Metallartefakte als ‚pitfalls' der Kernspintomographie. 72 Deutscher Röntgenkongress, Wiesbaden. ZBL Rad 143: 241
8. Zanella FE, Valavanis A (1994) Interventional neuroradiology of lesions of the skull base. Neuroimaging Clin North Am 4: 619–637
9. Virchow R (1856) Zur pathologischen Anatomie der Netzhaut und des Sehnerven. Virchows Arch Pathol Anat 10: 170–193
10. Weber AL (1992) Comparative assessment of diseases of the orbit using computed tomography and magnetic resonance imaging. Isr J Med Sci 28: 153–160
11. Dutton JJ (1992) Optic nerve sheath meningiomas. Surv Ophthalmol 37: 167–183
12. Som PM, Curtin HD (1996) Head and neck imaging, 3rd edn. Mosby, St Louis
13. Azar-Kia B, Naheedy MH, Elias DA, et al (1987) Optic nerve tumors: role of magnetic resonance imaging and computed tomography. Radiol Clin North Am 25: 561–581
14. Atlas SW, Grossman RI, Hackney DB, et al (1988) STIR MR imaging of the orbit. AJR 151: 1025–1030
15. Hart WM (1980) Bilateral optic nerve sheath meningioma. AJNR 1: 375
16. Daniels DL, Williams AL, Syvertsen A, et al (1982) CT recognition of optic nerve sheath meningioma: abnormal sheath visualization. AJNR 3: 181–183
17. Irnberger T (1985) High resolution computed tomography in primary and secondary lesions of the optic nerve sheath complex. RoFO Fortschr Geb Roentgenstr Nuklearmed 143: 151–157
18. Zimmerman CF, Schatz NJ, Glaser JS (1990) Magnetic resonance imaging of optic nerve meningiomas: enhancement with gadolinium-DTPA. Ophthalmology 97: 585–591
19. Lindblom B, Truwit CL, Hoyt WF (1992) Optic nerve sheath meningioma: definition of intraorbital, intracanalicular, and intracranial components with magnetic resonance imaging. Ophthalmology 99: 560–566
20. Dutton JJ (1991) Optic nerve gliomas and meningiomas. Neurol Clin 9: 163–177
21. Dutton JJ (1994) Gliomas of the anterior visual pathway. Surv Ophthalmol 38: 427–452
22. Taphoorn MJ, de Vries Knoppert WA, Ponssen H, Wolbers JG (1989) Malignant optic glioma in adults. J Neurosurg 70: 277–279
23. Herschey BL, Peyster RG (1987) Imaging of the cranial nerves: II. Semin Ultrasound CT MR 8: 164–176
24. Imes RK, Hoyt WF (1991) Magnetic resonance imaging signs of optic nerve gliomas in neurofibromatosis 1. Am J Ophthalmol 111: 729–734
25. Mafee MF, Putterman A, Valvassori GE, et al (1987) Orbital space-occupying lesions: role of computed tomography and magnetic resonance imaging. Radiol Clin North Am 25: 529–559
26. Atlas SW, Bilaniuk LT, Zimmerman RA, et al (1987) Orbit: initial experience with surface coil spin-echo MR imaging at 1.5 T. Radiology 164: 501–509
27. Haik BG, Saint-Louis L, Bierly J, et al (1987) Magnetic resonance imaging in the evaluation of optic nerve gliomas. Ophthalmology 94: 709–717
28. Kazim M, Kennerdell JS, Maroon J, Rothfus W, Marquardt M (1992) Choristoma of the optic nerve and chiasma. Arch Ophthalmol 110: 236–238
29. Azar-Kia B, Mafee MF, Horowitz SW, et al (1988) CT and MRI of optic nerve and sheath. Semin Ultrasound CT MR 9: 443–454
30. Rootman J (ed) (1988) Diseases of the orbit. JB Lippincott, Philadelphia
31. Mafee MF, Goldberg MF, Greenwald MJ, et al (1987) Retinoblastoma and simulating lesions: a role of CT and MR imaging. Radiol Clin North Am 25: 667–681
32. Haik BG, Smith ME, Ellsworth RM, et al (1986) Current diagnostic techniques in retinoblastoma. American Academy of Ophthalmology scientific exhibit, 9–13 November
33. Abramson DH, Ellsworth RM, Tretter P, et al (1981) Treatment of bilateral group I through III retinoblastoma with bilateral radiation. Arch Ophthalmol 99: 1761–1762
34. Char DH, Hedges TR, Norman D (1985) Retinoblastoma: CT diagnosis. Ophthalmology 92: 1143–1152
35. Char DH (1978) The management of small choroidal melanomas. Surv Ophthalmol 22: 377–387
36. Alvarez H, Rodesch G, Garcia-Monaco R, Lasjaunias P (1990) Embolization of the ophthalmic artery branches distal to its visual supply. Surg Radiol Anat 2: 293–297
37. Cummings BJ (1980) Relative risk factors in the treatment of juvenile nasopharyngeal angiofibroma. Head Neck Surg 3: 21–26
38. Dion JE (1992) Principles and methodology. In: Vinuela F, Halbach VV, Dion JE (eds) Interventional neuroradiology: endovascular therapy of central nervous system. Raven Press, New York, pp 1–15
39. Garcia-Monaco R, Lasjaunias P, Alvarez H, Rodesch G (1993) Embolization of vascular lesions of the head and neck. In: Valavanis A (ed) Interventional neuroradiology. Springer, Berlin Heidelberg New York, pp 1–22
40. Lasjaunias P (1980) Nasopharyngeal angiography: hazards of embolization. Radiology 136: 119–123
41. Lasjaunias P, Berenstein A (1987) Surgical neuroangiography, vol I: Functional anatomy of craniofacial arteries. Springer, Berlin Heidelberg New York
42. Valavanis A, Fisch U (1989) Juvenile nasopharyngeal angiofibroma: imaging, classification and embolization. In: Fisch U, Valavanis A, Yasargil MG (eds) Neurological surgery of the ear and skull base. Kugler and Ghedini, Amsterdam, pp 235–244
43. Debrun GM (1993) Endovascular treatment of carotid cavernous fistulas. In: Valavanis A (ed) Interventional neuroradiology. Springer, Berlin Heidelberg New York, pp 22–34
44. Valavanis A (1986) Preoperative embolization of the head and neck: indications, patient selection, goals and precautions. AJNR 7: 943–952

45. Jack CR Jr, Forbes G, Dewanjee MK, Brown ML, Earnest FN (1985) Polyvinyl alcohol sponge for embolotherapy: particle size and morphology. AJNR 6: 595–597
46. Kerber CW, Bank WP, Horton JA (1988) Polyvinyl alcohol foam: prepacking emboli for therapeutic embolization. Radiology 130: 1993–1994
47. Riche M, Hadjean E, Tran-Ba-Huy T, Merland J (1983) The treatment of capillary venous malformation using a new fibrosing agent. Plast Reconstr Surg 71: 607–612
48. Rodesch G, Lasjaunias P (1991) Embolization and meningiomas. In: Al-Mefti O (ed) Meningiomas. Raven Press, New York, pp 285–297
49. Zeumer H, Zanella FE (1993) Local intraarterial fibrinolysis in the vertebrobasilar and carotid territories. In: Valavanis A (ed) Interventional neuroradiology. Springer, Berlin Heidelberg New York, pp 159–172
50. Teasdale E, Patterson J, McLellan D, MacPherson P (1984) Subselective preoperative embolization for meningiomas: a radiological and pathological assessment. J Neurosurg 60: 506–511
51. Davis KR, Debrun GM (1987) Embolization of juvenile nasopharyngeal angiofibromas. Semin Intervent Radiol 4: 309–320
52. Gonzales G, Moret J (1990) Balloon occlusion of the carotid artery prior to surgery for neck tumors. AJNR 11: 649–652
53. Osguthorpe JD, Hochman M (1993) Inflammatory sinus diseases affecting the orbit. Otolaryngol Clin North Am 26: 657–671
54. Hudgins PA (1993) Complications of endoscopic sinus surgery: the role of the radiologist in prevention. Radiol Clin North Am 31: 21–32
55. Specht CS, Varga JH, Jalali MM, Edelstein JP (1992) Orbitocranial wooden foreign body diagnosed by magnetic resonance imaging. Dry wood can be isodense with air and orbital fat by computed tomography. Surv Ophthalmol 36: 341–344
56. Glatt HJ, Custer PL, Barrett L, Sator K (1990) Magnetic resonance imaging and computed tomography in a model of wooden foreign bodies in the orbit. Ophthalmic Plast Reconstr Surg 6: 108–114
57. Shih YY (1992) Inflammatory orbital pseudotomor. J Ophthalmic Nurs Technol 11: 258–262
58. McNicholas MM, Power WF, Griffin JF (1991) Idiopathic inflammatory pseudotumour of the orbit: CT features correlated with clinical outcome. Clin Radiol 44: 3–7
59. Flanders AE, Mafee MF, Rao VM, et al (1989) CT characteristics of orbital pseudotumors and other orbital inflammatory processes. J Comput Assist Tomogr 13: 40–47
60. Enzmann DR, Donaldson SS, Kriss JP (1979) Appearance of Graves' disease on orbital computed tomography. J Comput Assist Tomogr 6: 815–819
61. Forbes G, Gehring DG, Gorman CA, et al (1985) Volume measurements of normal orbital structures by computed tomographic analysis. AJNR 6: 419–424
62. Nugent MD, Belkin RI, Neigel JM, et al (1990) Graves' orbitopathy: correlation of CT and clinical findings. Radiology 177: 675–682
63. Hosten N, Schorner W, Lietz A, Wenzel KW (1992) The course of the disease in endocrine orbitopathy: magnetic resonance tomographic documentation. Rofo Fortschr Geb Rontgenstr Neuen Bildgeb Verfahr 157: 210–214
64. Niniaris N, Hurwitz JJ, Chen JC, Wortzman G (1994) Correlation between computed tomography and magnetic resonance imaging in Graves' orbitopathy. Can J Ophthalmol 29: 9–12